ChemComm

Accepted Manuscript

Volume 1 | Number 1 | Jan 2013 | Pages 1–100

ChemComm

Chemical Communications
www.rsc.org/chemcomm

ROYAL SOCIETY OF CHEMISTRY

ROYAL SOCIETY OF CHEMISTRY

www.rsc.org/chemcomm

ChemComm

ROYAL SOCIETY OF CHEMISTRY

Journal Name

COMMUNICATION

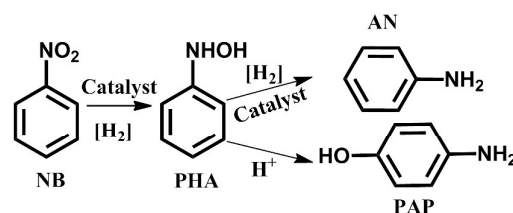### An Efficient Hydrogenation Catalyst in Sulfuric Acid for Nitrobenzene to *p*-Aminophenol: N-doped Carbon with Encapsulated Molybdenum Carbide

Tao Wang, Zhen Dong, Weimeng Cai, Yongzheng Wang, Teng Fu, Bin Zhao, Luming Peng, Weiping Ding∗ , and Yi Chen

1 **The transfer of catalytic function from molybdenum carbide to N-**
2 **doped carbon has tested by encapsulating the molybdenum**
3 **carbide with N-doped carbon in an one-pot preparation process.**
4 **The outer layer of N-doped carbon, inert itself, exhibits a high**
5 **activity and an excellent selectivity with the catalytic function**
6 **from molybdenum carbide for the hydrogenation of nitrobenzene**
7 **to *p*-aminophenol in sulfuric acid.**

Scheme 1. The catalytic hydrogenation of NB to PAP.

8 Carbides of transition metals with small carbon atoms in the
9 interstitial voids of the densely packed host lattice as non-
10 precious metal hydrogenation catalysts often show a similar or
11 surpassing catalytic properties when compared with the
12 precious metals such as Pd-, Pt- or Rh-based catalysts.[1] For
13 instance, molybdenum carbide has been proved to be an
14 excellent catalyst for plenty of hydrogenation-related
15 reactions such as hydrodeoxygenation,[2] hydrodesulfurization,
16 hydrodenitrogenation,[4] and hydrogenation of aromatic
17 compound.[5] However, molybdenum carbide itself may be not
18 appropriate for some hydrogenation reactions which need to
19 be conducted in a strong acid environment, such as the
20 hydrogenation of nitrobenzene (NB) to *p*-aminophenol (PAP).
21 Because molybdenum carbide could hardly survive from the
22 harsh condition of 10−15 wt. % sulfuric acid that is usually
23 necessary for rearrangement of phenyl hydroxylamine (PHA)
24 into PAP, otherwise, aniline would be the major production
25 (Scheme 1). Recently, a novel catalyst is designed and
26 prepared as N-doped carbon (CN) with underlying nickel and
27 the material could function well as a robust hydrogenation
28 catalyst for synthesis PAP from NB under strong acid
29 condition.[7] It has been demonstrated that CN becomes new
30 active sites for hydrogen adsorption and activation by
31 accepting electrons donated from the encapsulated nickel
32 which is successfully protected from corrosion in the reaction
33 system by CN at the same time.

34 Considering its unique metallic character with high electrical
35 and thermal conductivity as well as the outstanding electron-
36 donating ability, molybdenum carbides seem to be a better
37 candidate for the replacement of nickel. Recently, the
38 composites of molybdenum carbides and N-doped carbon
39 have been reported in fields such as electrode material for
40 lithium-ion batteries[8] and lithium-oxygen batteries[9] and
41 electrocatalysts for hydrogen generation reactions[10] with
42 excellent performances due to the strong interaction between
43 molybdenum carbides and N-doped carbon[8b] and synergistic
44 effect between molybdenum carbides and N dopants is
45 thought responsible for the high electrocatalytic activity[10b].
46 Furthermore, such a hybrid material is usually obtained based
47 on a solid reaction under an inert atmosphere different from
48 the temperature programmed reduction using mixture of
49 CH_4/H_2 [11] or merely H_2 [12] as reagents, making the process
50 simple and safe.
51 Herein we report a facile, one-pot route towards the
52 preparation of molybdenum carbides by an *in situ* solid
53 reaction under nitrogen atmosphere with molybdenum
54 chlorides[13] and urea as precursor while glucose is added for
55 the formation of CN at the same time according to the
56 report.[14] The material, denoted as CNMC, to the best of our
57 knowledge, is first used for catalytic hydrogenation of NB to
58 PAP in sulphuric acid with an excellent performance, indicating
59 the new design of catalyst with hydrogenation activity by CN
60 encapsulation is also applicative for molybdenum carbides
61 besides Fe, Co[15] and Ni.[16]

a. Key Lab of Mesoscopic Chemistry, School of Chemistry and Chemical Engineering, Nanjing University, Nanjing 210093, China. Email: dingwp@nju.edu.cn

ChemComm Accepted Manuscript
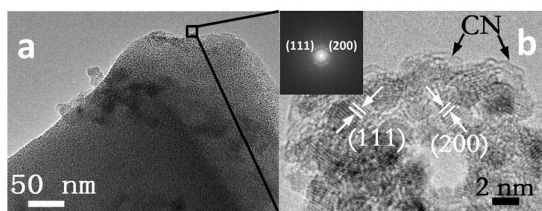
COMMUNICATION

Journal Name

Fig 1. (a) TEM and (b) HRTEM images of CNMC-2. Inset of b is the selected area electronic diffraction.
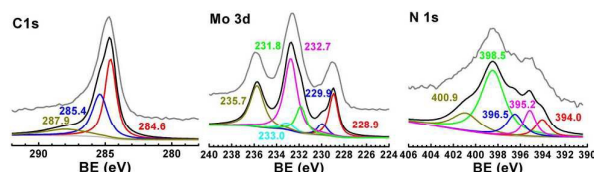
Fig. 2 XPS spectra of C 1s, N 1s and Mo 3d for CNMC-2. (The gray lines in the spectra give the original data).

Fig. 3 H−D exchange profiles of CNMC-2 and Ni/CN. Red line is the experimental data.

The as-prepared catalyst was characterized by various techniques to gain an insight into the crystallinity and morphology. As shown in Fig. S1, the material exhibits a characteristic diffraction peaks of metastable α−MoC$_x$ (2 θ = 36.6 ° and 42.6 ° for (111) and (200), respectively)[17] rather than stable Mo$_2$C, because it is said that α phase MoC$_x$ could be stabilized in a carbon-rich environment.[18] Moreover, a broad peak in the diffractogram at 23.7 ° could be assigned to (002) of the amorphous CN, which is further confirmed by Raman spectrum with a I_D/I_G value of 0.94. The presence of CN are also clearly displayed in the HRTEM image in Fig 1b with several layers surrounding MoC$_x$ particles which show a size distribution around 2 nm with high dispersity (Fig S2, ESI†). The catalyst shows a plate-like morphology according to the TEM image (Fig 1a) and SEM image (Fig S3, ESI†) and the uniform distribution of Mo is illustrated by EDX elemental mappings (Fig S3, ESI†).

X-ray photoelectron spectroscopy (XPS) experiments are carried out for chemical state of component elements and the results are displayed in Fig. 2. C1s peak could be deconvoluted into three peaks with binding energies at approximately 284.6, 285.4 and 287.9 eV. The peak at 284.6 eV is identified graphitic sp^2-bonded carbon[19] and the signal at 285.4 eV is ascribed to carbon atoms single bonded to nitrogen atoms[20] while the peak with the highest binding energy at 287.9 eV corresponds to carbon atoms that have one double and two single bonds with the nitrogen atoms[21]. As shown in N 1s spectrum, the peak located at 398.5 eV is ascribed to sp^2 hybridized aromatic N atoms bonded to carbon atoms (pyridinic nitrogen)[22] and the other peak at 400.9 eV is related to graphitic nitrogen[23]. Meanwhile, the signal at 394.0 eV is ascribed to Mo 3p$_{3/2}$[24] and the other two peaks at 395.2 eV and 396.5 eV correspond to anionic N-doping where O is replacement by N atoms according to previous reports[25], indicating a strong interaction between Mo and N. Furthermore, the spectrum of Mo 3d exhibits six peaks, which are assigned to 3d$_{5/2}$ (232.7 eV) and 3d$_{3/2}$ (235.7 eV) of Mo^{6+}, 3d$_{5/2}$ (229.9 eV) and 3d$_{3/2}$ (233 eV) of Mo^{4+}, as well as 3d$_{5/2}$ (228.9 eV) and 3d$_{3/2}$ (231.8 eV) of Mo–C,[26] which accounts for about 28 % of the Mo species. In order to give an accurate content of carbon, nitrogen and hydrogen, elemental analysis is carried out, and the results are shown in Table S1 (ESI†). Carbon exhibits a high proportion about 38 wt. % and nitrogen accounts for nearly 1.8 wt. % while the content of hydrogen is 0.88 wt. %. The mass fraction of Mo in the catalyst is determined according to the result of thermal gravity analysis
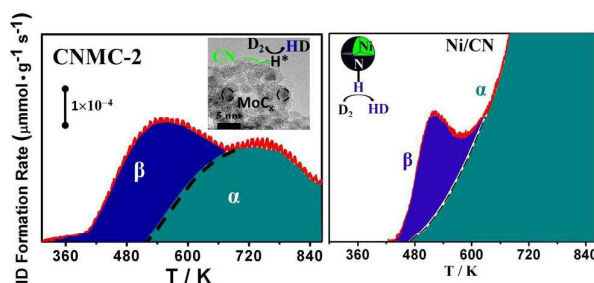
(TGA) for the catalyst showed in Fig. S4 (ESI†). There is a weight increase in the curve occurred at ca. 350−450 °C, which could be attributed to the oxidation of MoC$_x$ with the presence of oxygen.[27] The weight loss beginning at about 500 °C is resulted from the decomposition of CN and the platform at 600−800 °C indicates that CN has been decomposed completely with a residual of MoO$_3$ (63.0 wt. %). Therefore, content of Mo in the material is calculated to be 42 wt. % and thus O accounts for ~17 wt. %, spontaneously.

According to the result of hydrogen/deuterium (H−D) exchange experiment shown in Fig. 3, surface adsorbed hydrogen of CNMC-2 is discussed with the previously reported Ni/CN[7b]. It could be seen that H−D exchange begins at a lower temperature for CNMC-2 than that of Ni/CN, indicating its higher activity. Hydrogen species α with a peak temperature at 750 K is identified as hydrogen tightly bonded to CN according to the reports[7]. Meanwhile, the peak located at 547 K detected as hydrogen species β could be assigned to the activated hydrogen for catalytic hydrogenation of nitrobenzene based
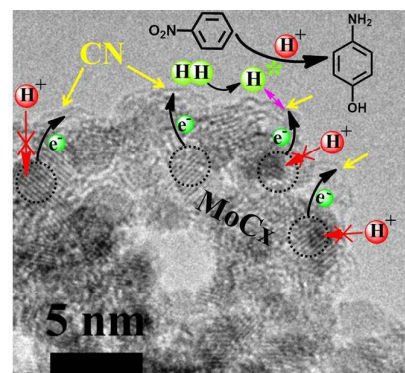

Fig. 4 Schematic diagram of catalytic hydrogenation of NB to PAP with CNMC-2.

Journal Name

COMMUNICATION

Table 1 Catalytic performance of catalysts for catalytic hydrogenation of NB to PAP.

Entry	Catalyst [a]	Solvent	Temp. (°C)	Conv. (%)	Sel. (%)
1	CNMC-1	H_2O	120	100	– [b]
2	CNMC-1	1.5 M H_2SO_4	120	94.3	25.2
3	CNMC-1	1.5 M H_2SO_4	100	77.9	80.8
4	CNMC-1	1.5 M H_2SO_4	80	51.9	87.9
5	CNMC-2	1.5 M H_2SO_4	100	68.1	91.8
6	CNMC-3	1.5 M H_2SO_4	100	47.5	> 99
7	CNMC-4	1.5 M H_2SO_4	100	77.1	64.2
8	CNMC-5	1.5 M H_2SO_4	100	84.2	35.1
9	MC	1.5 M H_2SO_4	100	36.3	75.5
10	CN	1.5 M H_2SO_4	100	–	–
11	Ni/CN [7b]	1.5 M H_2SO_4	120	43	> 99

[a] The different catalysts are prepared with a series CN loading by adding a various amount of glucose in the synthesis CNMC and the details are displayed in the supporting information.
[b] Aniline is the only product.

on the previous work[7]. Moreover, XRD pattern confirms the phase of MoC_x after H/D exchange experiments (Fig. S5, ESI†) indicating that the catalyst sample doesn't suffer phase change.

As described in the schematic diagram of the catalytic hydrogenation of NB to *p*-aminophenol with CNMC (Fig. 4), molybdenum carbides endow CN with the ability for hydrogen adsorption and activation by denoting electrons to CN, making it active for catalytic hydrogenation reactions and it is reported that N-doped carbon is responsible for H_2 activation[28]. Meanwhile, molybdenum carbide is isolated from the strong acid condition which is necessary for hydrogenation of NB to aminophenol. The catalytic performance of CNMC is listed in Table 1. Entry 1 and 2 show the catalytic results of CNMC-1 with different solvent, indicating that a strong acid environment is certainly necessary for the formation of aminophenol. Entries 2−4 provide the catalytic performance of CNMC-1 conducted at different temperature and therefore the optimal condition is set to be 373 K when taking both NB conversion and PAP selectivity into account. Meanwhile, effect of CN loading is also investigated by adjusting the quantity of glucose in the synthesis process. As illustrated in the results of TGA analysis for the as prepared catalysts (Fig S6, ESI†), CNMC-1 possesses the lowest CN loading, while CNMC-3 exhibits the highest CN loading. According to the results listed in Table 1, CNMC-3 exhibits the poorest catalytic activity but the highest PAP selectivity while CNMC-1 shows the highest NB conversion but the lowest PAP selectivity, because it is reported that thinner CN shell which is benefit for electron transfer would result in a higher catalytic activity[29]. Extremely, catalyst MC obtained without an addition of any glucose does possess a lower catalytic activity due to the surrounding CN obtained from decomposition of urea with the aid of the catalytic performance of Mo species for growth of carbon[26b] and it is clearly displayed in the HRTEM image of MC (Fig. S7, ESI†), however, it could not be reused for even one more time,
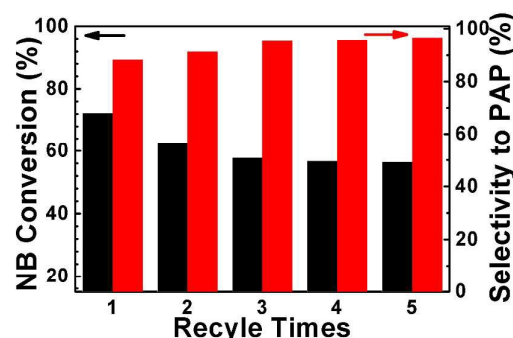

Fig. 5 Recyclable catalytic hydrogenation of NB to PAP with CNMC-2.

because MoC_x would gradually dissolve in the strong acid condition without the protection from robust carbon nitride made from glucose, only left a little residual carbon. In contrast, pure CN does not show any catalytic activity, indicating that presence of MoC_x is essential for such a CN encapsulated catalyst to be an electron donor. In conclusion, CNMC-2 seems to be the most appropriate candidate for the hydrogenation reaction and it does show a higher catalytic activity even when the catalytic hydrogenation reaction is conducted at a lower temperature than the reported Ni/CN (Entry 11). Given the poor surface specific area (SSA) of CNMC-2 (1.9 $m^2\,g^{-1}$) that calculated from its N_2 adsorption−desorption isotherm using the Brunauer−Emmett−Teller (BET) method (Fig. S8, ESI†), effects of SSA are studied by adjusting the mass ratio of urea and glucose to 10/1 and 40/1 and SSA for the two samples is calculated to be 28 $m^2\,g^{-1}$ (CNMC-4) and 121 $m^2\,g^{-1}$ (CNMC-5), respectively (Fig. S9, ESI†). Their catalytic performances are displayed in entry 7 and entry 8 in Table 1, NB conversion shows an increasement from 64.8 % to 84.2 %, however PAP selectivity decreases from 91.8 % to 35.1 % with increasing SSA from CNMC-2 to CNMC-5, which may be ascribed to the strong adsorption of NB and PHA on catalyst surface, inclined to a further hydrogenation of PHA. Additionally, a recycle test for CNMC-2 is conducted for a better understand of its stability. As shown in Fig. 5, CNMC-2 still possesses a NB conversion about 50 % and PAP selectivity is calculated to be 96.6 % even when used for 5 times, which is a indicative of its high stability. The deactivation may result from adsorption of substances on the surface of catalyst through π−π interaction considering that both N-doped carbon and organic compounds in the reaction system are characterized with aromatic properties and content of carbon shows an increase by 1.4 wt. % for the spent catalyst in Table S2 (ESI†) compared with the fresh one. Furthermore, corrosion of the catalyst under such a harsh condition is estimated by inductively coupled plasma (ICP) investigation and concentration of Mo in the solution which is diluted to a constant volume (100.0 mL) after reaction is measured to be 2.49 ppm and thus Mo content of the spent catalyst is estimated to be 39.0 wt. %, a slightly lower than that of the fresh one.

COMMUNICATION

Moreover, XPS tests are carried out to study chemical state of component elements for spent CNMC-2. As listed in the Mo 3d core level spectrum (Fig. S10, ESI†), there are six peaks which are ascribed to $3d_{5/2}$ (232.6 eV) and $3d_{3/2}$ (235.7 eV) of Mo^{6+}, $3d_{5/2}$ (229.6 eV) and $3d_{3/2}$ (233 eV) of Mo^{4+}, as well as $3d_{5/2}$ (228.8 eV) and $3d_{3/2}$ (231.8 eV) of Mo–C, which accounts for about 31.3 % of Mo species and the results are in well consistent with the fresh one, suggesting that the catalyst is efficiently protected by CN from the acid corrosion. Meanwhile spectra of C 1s and N 1s show little changes from the as prepared catalyst, indicating a high stability of CN. And it is further demonstrated by elemental analysis for carbon, nitrogen and hydrogen of the spent catalyst (Table S2 ESI†). Compared with the fresh catalyst, the spent one shows comparative composition. Therefore, O accounts for 19.0 wt.% in the spent catalyst. Furthermore, the crystallization and particle size of spent CNMC-2 almost keep the same with the as-prepared one based on the TEM and HRTEM images (Fig. S11, ESI†) and the crystal phase of α-MoC_x in the used catalyst is further confirmed by its XRD spectrum (Fig. S12, ESI†).

In summary, although molybdenum carbides exhibit a high catalytic activity for hydrogenation reactions, it could hardly maintain its structure in a strong acid environment and also it would be oxidized into molybdenum oxide rapidly when exposed to ambient atmosphere without any passivation. Here a novel structure of molybdenum carbides as an acid-resistant hydrogenation catalyst is designed and prepared by N-doped carbon encapsulation through a solid reaction. The catalyst with a robust structure shows excellent stability in sulphuric acid for the one-pot hydrogenation of nitro-benzene to aminophenol with a high catalytic activity. The unique construction would pave the way for designs of functional catalysts with promising properties distinguished from those in traditional structures.

Notes and references

1 (a) J.G. Chen, *Chem. Rev.*, 1996, **96**, 1477; (b) H.H. Hwu and D.Y. Zhao, *Chem. Rev.*, 2005, **105**, 185; (c) R.J. Hou, K. Chang, J.G. Chen and T.F. Wang, *Top Catal.*, 2015, **58**, 240; (d) S.T. Oyama, *Catal. Today*, 1992, **15**, 179.

2 (a) H. Ren, W.T. Yu, S. M. Salciccioli, Y. Chen, Y.L. Huang, K. Xiong, D.G. Vlachos and J.G. Chen, *ChemSusChem*, 2013, **6**, 798; (b) R. Ma, K. Cui, L. Yang, X.L. Ma and Y.D. Li, *Chem. Commun.*, 2015, **51**, 10299.

3 (a) B. Dhandapani, T.St. Clair and S.T. Oyama, *Appl. Catal.*, 1998, **168**, 219; (b) P.A. Aegerter, W.C. Quigley, G.J. Simpson, D.D. Ziegler, J. W. Logan, K.R. McCrea, S. Glazier and M.E. Bussell, *J. Catal.*, 1996, **164**, 109.

4 J.G. Choi and L.T. Thompson, *J. Catal.*, 1995, **154**, 33.

5 (a) J.S. Lee, M.H. Yeom, K.Y. Park, I.S. Nam, J.S. Chung, Y.G. Kim and S.H. Moon, *J. Catal.*, 1991, **128**, 126; (b) M. Frauwallner, F. López-Linares, J. Lara-Romero, E. Hernández and P. Pereira-Almao, *Appl. Catal. A*, 2011, **394**, 62; (c) N. Perret, X. D. Wang, C. Potvin, C. Louis, M. A. Keane, *J. Catal.*, 2012, **286**, 172; (d) G. Vitale, H. Guzmán, M. L. Frauwallner, E. Scott, P. Pereira–Almao, *Catal. Today,* 2015, **250**, 123.

6 (a) C.O. Henke and J.V. Vaughen, US Patent, 1940, 2198249; (b) R.G. Bennern, US Patent, 1968, 3383416.

7 (a) T. Fu, M. Wang, W.M. Cai, W. Chen and W.P. Ding, *ACS Catal.*, 2014, **4**, 2536; (b) T. Wang, Z. Dong, T, Fu, Y.C. Zhao, T.

8 (a) Q. Gao, X.Y. Zhao, Y. Xiao and M.H. Cao, *Nanoscale*, 2014, **6**, 6151; (b) R.R. Li, S.G. Wang, W. Wang and M.H. Cao, *Phys. Chem. Chem. Phys.*, 2015, **17**, 24083.

9 W.J. Kwak, K.C. Lau, C.D. Shin, K. Amine, L.A. Curtiss and Y.K. Sun, *ACSNano*, 2015, **9**, 4129.

10 (a) K. Zhang, Y, Zhao and Y.J. Chen, *J. Mater. Chem. A,* 2015, **3**, 5783; (b) Y.P. Liu, T. Asefa, W. Chen and X.X. Zou, *Angew. Chem. Int. Ed.*, 2015, **54**, 10752; (c) K. Zhang, C.Y. Li, X.B. Yu and Y.J. Chen, *Phys. Chem. Chem. Phys.*, 2015, **17**, 16609.

11 (a) J.S. Lee, S.T. Oyama and M. Boudart, *J. Catal.*, 1987, **106**, 125; (b) X.W. Chen, T. Zhang, P.L. Ying, M.Y. Zheng, W.C. Wu, L.G. Xia, X.D. Wang and C. Li, *Chem. Commun.*, 2002, 288.

12 (a) X.Y. Li, D. Ma and X.H. Bao, *Catal. Lett.*, 2007, **116**, 63; (b) C.H. Liang, P.L. Ying and C. Li, *Chem. Mater.*, 2002, **14**, 3148.

13 (a) C. Giordano, C. Erpen, W.T. Yao and M. Antonietti, *Nano Lett.*, 2008, **8**, 4659; (b) D.P. Xiang, Y. Liu, S.J. Gao and M.J. Tu, *J. Mater. Charact.*, 2008, **59**, 241; (c) L. Ma, L.R. Ting, V. Molinari and B.S. Yeo, *J. Mater. Chem. A*, 2015, **3**, 8361.

14 X.H. Li, S. Kurasch, U. Kaiser and M. Antonietti, *Angew. Chem. Int. Ed.*, 2012, **51**, 9689.

15 D.F. Su, Z..Z.. Wei, S.J. Mao, J. Wang, Y. Li, H.R. Li, Z..R. Chen and Y. Wang, *Catal. Sci. Tech.*, 2016, **6**, 4503.

16 (a) R.V. Jagadeesh, A. Surkus, H. Junge, M. Pohl, J. Radnik, J. Rabeah, H.M. Huan and M. Beller, *Science*, 2013, **342**, 1073; (b) F.A. Westerhaus, R.V. Jagadeesh, G. Weienhofer, M. Pohl, J. Radnik, A. Surhus , M. Nielsen, A. Bruckner and M. Beller, *Nat. Chem.*, 2013, **5**, 537.

17 R. Kojima and K. Aika, *Appl. Catal. A: Gen.*, 2001, **219**, 141..

18 (a) H. Preiss, B. Meyer and C. Olschewski, *J. Mater. Sci.*, 1998, **33**, 713; (b) M. Pang, X. Z. Chen, Q.Y. Xu and C.H. Liang, *Appl. Catal. A: Gen.*, 2015, **490**, 146.

19 (a) C. Ronning, D. Schwen, S. Eyhusen, U. Vetter and H. Hofsäss, *Surf. Coat. Tech.*, 2002, **158**, 382; (b) J. Schäfer, J, Ristein, R. Graupner and L. Ley, *Phys. Rev. B*, 1996, **53**, 7762.

20 W.J. Si, J. Zhou, S.M. Zhang, S.J. Li, W. Xing and S.P. Zhuo, *Electrochim. Acta*, 2013, **107**, 397.

21 A.P. Dementjev, A. Graaf, M.C.M. Sanden, A.V. Naumkin and A.A. Serov, *Diamond Relat. Mater.*, 2000, **9**, 1904.

22 (a) Y. Zheng, Y. Jiao, L. Ge, M. Jaroniec and S.Z. Qiao, *Angew. Chem. Int. Ed.*, 2013, **52**, 3110; (b) J.H. Liu, T.K. Zhang, Z.C. Wang, G. Dawson and W. Chen, *J. Mater. Chem.*, 2011, **21**, 14398; (c) T.Y. Ma, S. Dai, M. Jaroniec and S.Z. Qiao, *Angew. Chem. Int. Ed.*, 2014, **53**, 7281.

23 (a) R. Arrigo, M. Hävecker, R. Schlögl and D.S. Su, *Chem. Commun.*, 2008, 4891; (b) S.P. Wang, J. Wang, B.Y. Xiao, D.F. Su, H.R. Li and Y. Wang, *J. Am. Chem. Soc.*, 2015, **137**, 15753.

24 R. Nyholm and N. Martensson, *J. Phys. C: Solid St. Phys.*, 1980, **13**, L279.

25 (a) N. Selvakumar, K. Rajaguru, G.M. Gouda and H.C. Barshilia, *Sol. Energy*, 2015, **119**, 114; (b) R. Asashi, T. Morikawa, T. Ohwaki, K. Aoki and Y. Taga, *Science*, 2001, **293**, 269; (c) Q. Xiao, L.L. Quyang, L. Gao and C. Yao, *Appl. Surf. Sci.*, 2011, **257**, 3652; (d) H. Wang, H.P. Ho, K.C. Lo and K.W. Cheah, *Mater. Chem. Phys.*, 2008, **107**, 244.

26 (a) G. Vitale, H. Guzmán, M. Frauwallner, C.E. Scott and P. Pereira-Almao, *Catal. Today*, 2015, **250**, 123; (b) J.Y. Qiu, Z.X. Yang and Y. Li, *J. Mater. Chem. A*, 2015, **3**, 24245.

27 (a) D. Zhou, H.P. Wu, and B.H. Han, *Phys. Chem. Chem. Phys.*, 2013, **15**, 16898; (b) R.G. Ma, Y. Zhou, Y.F. Chen, P.X. Li, Q. Liu and J.C. Wang, *Angew. Chem., Int. Ed.*, 2015, **54**, 14723.

28 Z..Z.. Wei, J. Wang, S.J. Mao, D.F. Su, H.Y. Jin, Y.H. Wang, F. Xu, H.R. Li and Y. Wang, *ACS Catal.* 2015, **5**, 4783.

29 J. Deng, P.J. Ren, D.H. Deng and X.H. Bao, *Angew. Chem. Int. Ed.*, 2015, **54**, 2100.